ISSN: 2689-1204

Research Article

Journal of Applied Material Science & Engineering Research

# Crystallization, Dielectric, and Energy Storage Properties of Phosphate Glass–Ceramics

**Abderrahim Ihyadn[1*], Daoud Mezzane[2], M'barek Amjoud[1], Abdelilah Lahmar[2], Lahcen Bih[4,5], Abdelhadi Alimoussa[1], Igor Luk'yanchuk[2,3] and Mimoun El Marssi[2]**

*[1]IMED-Lab, Cadi Ayyad University, Morocco*

*[2]LPMC, University of Picardy Jules Verne, France*

*[3]Department of Building Materials, Kyiv National University of Construction and Architecture, Ukraine*

*[4]Materials and Processes Department, ENSAM Meknes, Moulay Ismail University, Morocco.*

*[5]Physico-Chemistry Condensed Matter Team (PCMC), Faculty of Sciences of Meknes, Moulay Ismail University, Morocco*

**[*]Corresponding Author**
Abderrahim Ihyadn, IMED-Lab, Cadi Ayyad University, Morocco

**Submitted:** 2024, Feb 07; **Accepted:** 2024, Feb 27; **Published:** 2024, Mar 05

**Citation:** Ihyadn, A., Mezzane, D., Amjoud, M. B., Lahmar, A., Bih, L., et. al. (2024). Crystallization, dielectric, and energy storage properties of phosphate glass–ceramics. *J App Mat Sci & Engg Res, 8*(1), 01-09.

## Abstract

*The $BaO$-$Na_2O$-$Nb_2O_5$-$WO_3$-$P_2O_5$ glass-ceramics were synthesized using a melt-quenching technique coupled with a controlled crystallization process. It was found that increasing crystallization temperature promoted the increase of ceramic phases precipitated and the average grains size of glass-ceramics, resulting in the increase of the dielectric constant. The large dielectric constant of 315 was achieved for glass crystallized at 1000°C. In addition, a thermally stable dielectric constant was noticed in the temperature range from 25 °C to 250 °C. Low dielectric losses below 0.04 were obtained for all samples. The recoverable energy density (Wrec) was enhanced as the crystallization temperature increased. The sample heated at 1000°C exhibited a high Wrec of 177mJ/cm$^3$ with an energy efficiency of 73.8% under 120 kV/cm. These results suggest that phosphate glasses based on niobate glass-ceramics are a promising material for pulse capacitors.*

**Keywords:** Glass-Ceramic; Phosphates; Crystallization Temperature; Dielectric; Energy Storage Density.

## 1. Introduction

In recent years, high power density dielectric capacitors with ultrafast charge-discharge speed have seen extensive applications in pulse power systems such as those used in the military sector, hybrid automobiles, and for the storage of renewable energy [1–3]. The low energy storage density of dielectric capacitors limits their further development with respect to fuel cells and batteries. [4,5]. Hence, increasing the dielectric energy storage density is now a serious obstacle for scientists to surmount. Dielectric ceramics and polymer-based dielectrics are the two primary types of energy storage materials [6,7]. Although dielectric ceramics have a high permittivity, they generally display a relatively low breakdown strength (BDS) [8,9]. Conversely, polymer-based dielectrics generally provide high BDS, but they maintain low dielectric constant and poor thermal stability [10,11].

In this regard, the major emphasis of research has been on dielectric glass-ceramics, which are characterized as composite materials that combine the benefits of ceramic phase and glass matrix [7]. Crystal phases could substantially improve the permittivity, and glass networks can enhance BDS. [12,13]. Despite being classified as linear dielectric materials, glass-ceramics have an energy storage density related to the square of the BDS and the dielectric constant [1,7]. In the present glass-ceramics system, the formation of the ceramic phase is constrained by the dense glass network structure, which results in a high BDS and low permittivity. As a result, the achievement of an optimum energy storage density is limited. Hence, it is more likely to enhance both the dielectric constant and BDS.

The emphasis of glass-ceramics research focuses primarily on niobate-based glass systems [7,14]. By controlling the content of the glass forming and the precipitation phase during the crystallization process, the grain size and content of the ceramic phase with high dielectric constant can be efficiently controlled,

so the energy storage may be improved [15,16]. Wang et al. investigated the influence of nucleating agents (CeO2, ZrO2, and CaF2) on the energy storage density of KSN-based glass-ceramics. They revealed that the addition of 3 mol% CaF2 promoted the precipitation of the crystalline phase with high permittivity, and they optimized the dielectric constant and breakdown strength [17].

Recently, (BaO,Na2O)-Nb2O5 with different glass phase formation has been studied from the phase ratio, crystallization time, interface polarization, and discharged property [15,18]. Likewise, the permittivity of glass-ceramics can be increased by adopting a higher crystallization temperature. Tao Jiang et al. reported the effect of crystallization temperature on the phase development of 21.25BaO–1PbO-12.75Na2O–34Nb2O5–32SiO2 and reported that the relative permittivity progressively rose due to the formation of phases with high dielectric constant [19]. Kaikai Chen reported that when BaO-Na2O-Bi2O3-Nb2O5-Al2O3-SiO2 glass- ceramics were crystallized at higher temperatures, the discharged energy density increased, reaching an optimal discharge energy density of 0.48 J/cm3 for the sample crystallized at 950°C [20]. In our previous findings, we showed. that increasing the crystallization temperature improved the dielectric permittivity and the energy storage density of BaO-NaO-Nb2O5-P2O5 glass-ceramics [21].

Moreover, Ihyadn et al investigated the effect of WO3/Nb2O5 on the performance of a BaO- Na2O-Nb2O5-P2O5 glass-ceramic system and found that raising the WO3 content resulted in high energy efficiency [22]. In present work, BaO-Na2O-Nb2O5-WO3-P2O5 (BNNWP) glass- ceramics were crystallized at different temperatures. The phase evolution, microstructure, dielectric performances, impedance spectroscopy, and energy storage properties were investigated in various heating temperatures in order to find the optimum crystallization temperature of BNNWP glass-ceramics.

## 2. Experimental Procedures

The33.3BaO-8.3Na2O-33.36Nb2O5-8.34WO3-16.7P2O5 (BNNWP) glass system was synthesized via the quenching method as reported in our previous work [22]. In addition, the BNNWP glasses were crystallized at different temperatures 760°C, 800°C, 900°C and 1000°C, and designated as B760, B800, B900, and B1000 respectively. The samples were crystallized in the air for 10 h with a heating rate of 10 ◦C/min based on DSC results.

The characterization techniques used for investigating the structural, microstructural, and dielectric properties were cited in our previous work [21]. The energy storage properties were studied using the CPE1701, PolyK, USA, with a high voltage power supply (Trek 609-6, USA). For the P–E measurement, silver electrodes with a 13 mm diameter and 0.25 mm thickness were coated on the two sides of the samples.

## 3. Results and Discussion

### 3.1 Phase Evolution and Microstructure

The DSC result of the BNNWP glass sample acquired at a heating rate of 10 °C min is shown in Figure 1. Additionally, two exothermic peaks, Tp1 and Tp2, are seen on DSC plots. Tp1 is located at 735°C, while Tp2 is around 827°C. Such two anomalies are evidence that two ceramic phases within the glass matrix were formed.

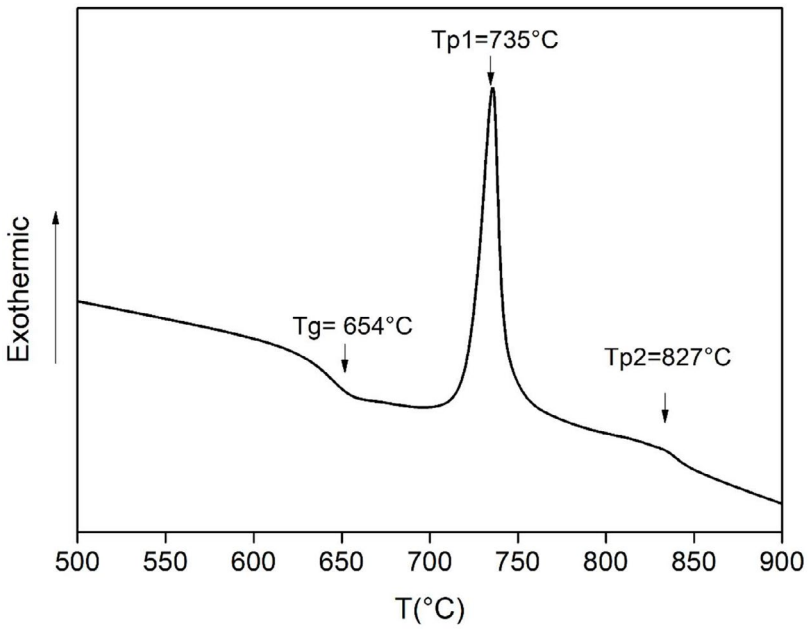


**Figure 1:** Differential Scanning Calorimetry (DSC) curves for BNNWP glass

Figure 2 depicts the phase evolution of BNNWP glass-ceramics at various crystallization temperatures. According to the XRD patterns, two main phases were formed: Ba2NaWNb4O15, which is a tetragonal tungsten bronze structure, and NaNbO3 in which the perovskite structure is cubic. Additionally, it is noticed that the peaks intensity of XRD analysis increases as the crystallization temperatures rise. These findings may suggest an increase in the dielectric constant as the heat treatment temperature rises. Similar results have been observed elsewhere [14,19].

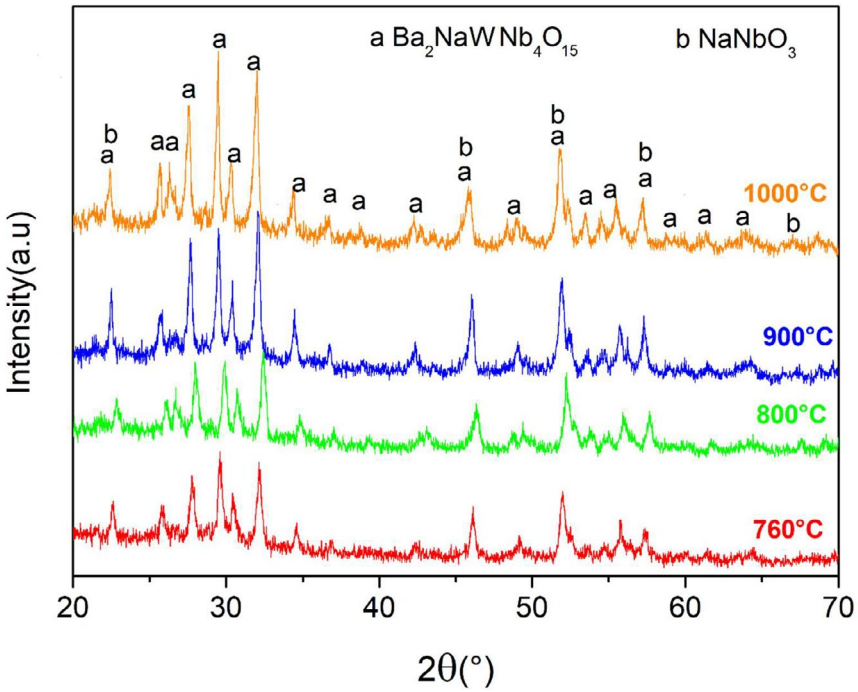


**Figure 2:** XRD patterns of the BNNWP glass-ceramics at different crystallization temperatures

Figure 3 displays SEM images of BNNWP glass-ceramics. The microstructure of the glass- ceramics is homogenous and dense, with regular grain shapes and uniform grain size distributions. In addition, the white particles observed for B1000 could be attributed to impurity phase emerging at a high crystallization temperature. It is observed that the average grain increases as the crystallization temperature increases. Glass-ceramics crystallized at 760°C, 800°C, 900°C and 1000°C present an average grain size of 1.3µm, 1.5µm, 1.7µm, and 2µm, respectively. The average grain size was calculated by Image J. Large grain sizes can promote polarization, which can improve the dielectric constant. However, it may result in a loss in BDS because of charges accumulating at grain boundaries as a result of the huge disparity between large grain size and glass matrix [23].

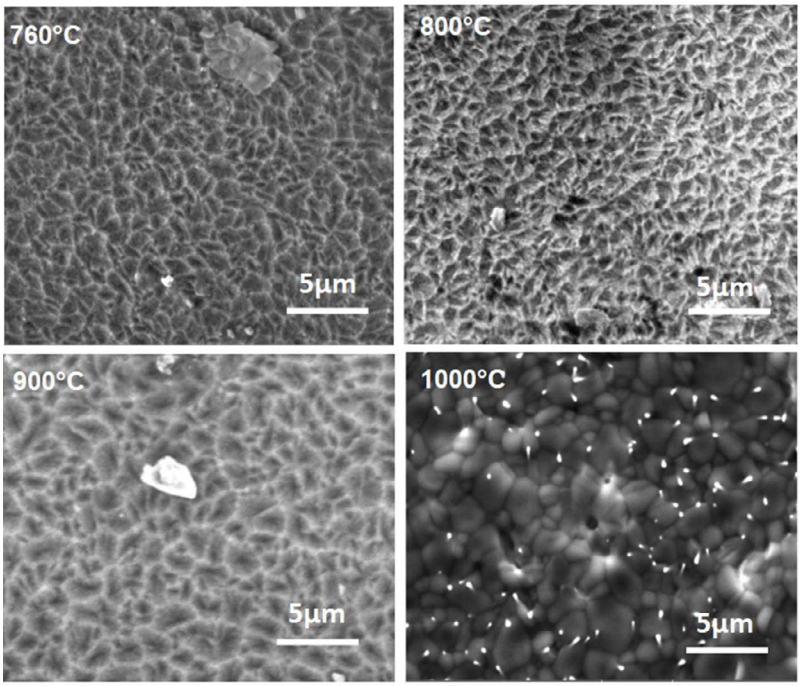


**Figure 3:** SEM images of BNNWP samples crystallized at different temperatures

### 3.2 Dielectric Investigations

The thermal variation of the dielectric constant and dielectric losses of BNNWP glass-ceramics is illustrated in Fig. 4. It is evident that an increase in crystallization temperature increases the samples' dielectric constant. For instance, it rises from 65 to 100, and 218 and 315 at 760°C, 800°C, 900, and 1000°C,

respectively. This result could be explained by an increase of ferroelectrics phases Ba2NaWNb4O15 (εr=100-300) and NaNbO3 phases (εr= 500-600) with highεr, as the crystallization temperature increases according to XRD results [19,20,24-26]. Furthermore, it should be noticed that this rise correlated with increased of the grain size detected in the SEM results. In addition, the significant thermal stability of the dielectric constant with a rate of variation less than 3% was noticed in the temperature range of 25°C to 250°C for all samples except for B1000. Dielectric capacitors are typically employed at various ambient temperatures. The outstanding thermal stability of this material is therefore of great practical importance for technical applications. Furthermore, the dielectric loss reduces with increasing crystallization temperature and eventually increases for B1000. It passes from 0.017 to 0.008, and 0.011, and 0.038 for B760, B800, B900, and B1000, respectively at Room temperature. Despite this, the dielectric loss remains less than 0.04 for all the samples due to the defect-free quality of the glass phase.

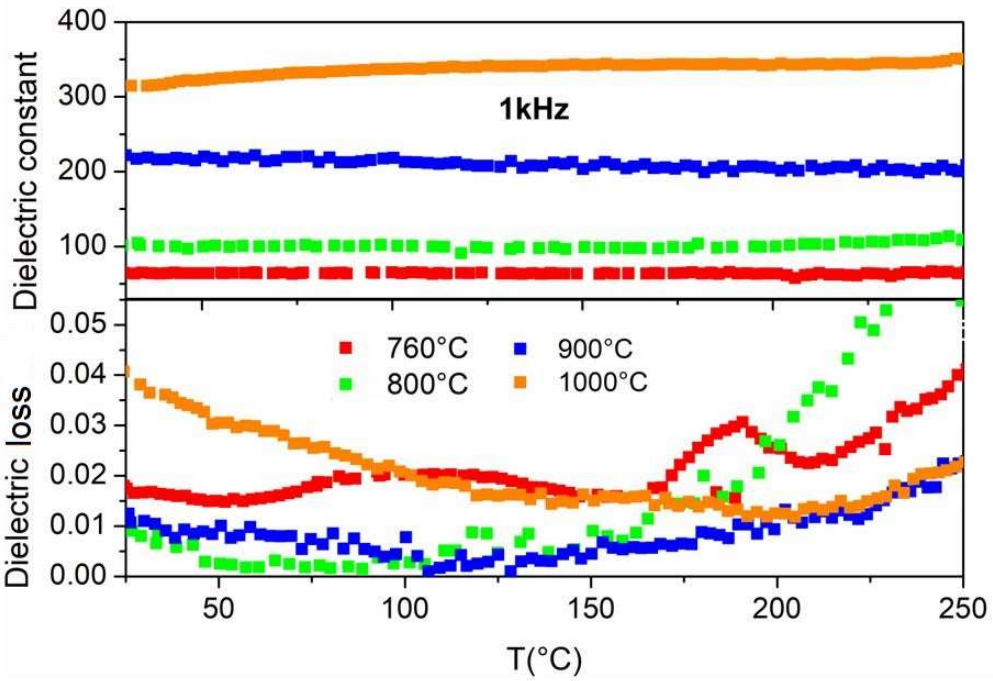


**Figure 4:** Thermal variation of dielectric constant and loss of BNNWP samples at 1kHz

Figure 5 depicts the frequency-dependence of the dielectric constant of BNNWP glass-ceramics at room temperature. Except for B1000, all samples exhibit good frequency stability of dielectric permittivity, which is advantageous for capacitor applications [27].

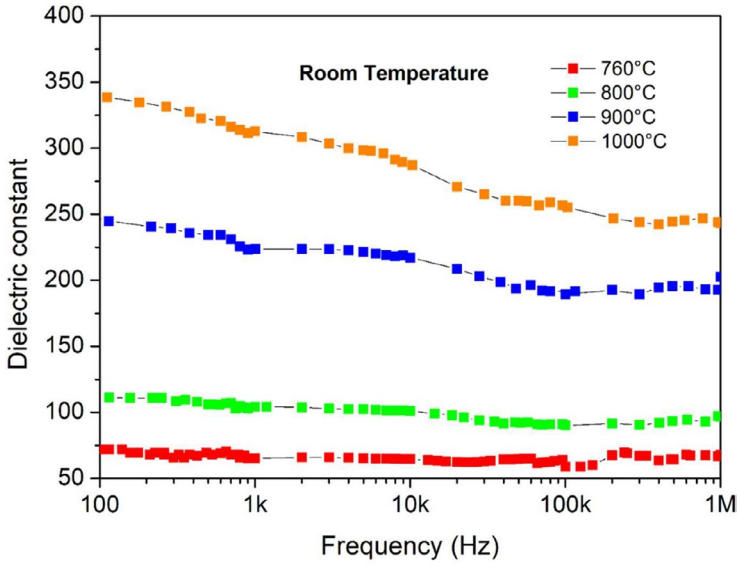


**Figure 5:** Frequency-dependence of dielectric permittivity Room temperature

### 3.3 Impedance Spectroscopy

Figure 6 displays the complex impedance spectrum of B760 glass-ceramic from 400°C to 480°C, with a range of 20°C. A simple parallel resistance-capacitance R-C circuit was used to simulate the contributions of the grain and grain boundary of the samples. The area of the curve declines as the test temperature increases, revealing that the impedance of the glass-ceramic decreases. This could be attributed to the thermal activation of defects generated by Maxwell– Wagner interface relaxation originating from the interaction of grains and glass matrix [28]. As illustrated in the inset of Fig. 6, the equivalent circuit is represented utilizing two R-C elements connected in series. ZVIEW® was deployed to fit our experimental results.

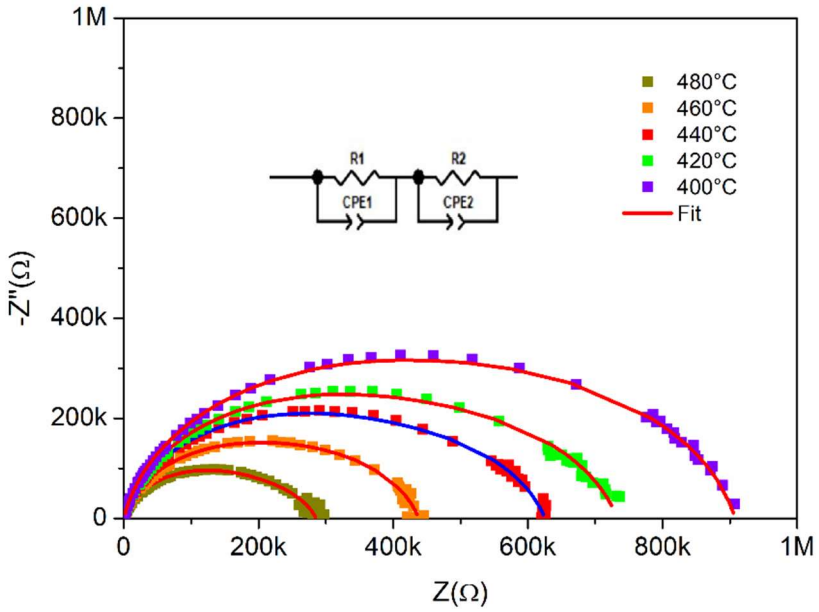


**Figure 6:** Complex impedance spectrum of B760 sample

The impedance plots of all samples BNNWP at 460°C are presented in figure 7. For the analyzed frequency range (20Hz-1MHz), a good fitting of the experimental results was obtained for all samples. For each observed arc, two contributions from the glass phase and ceramic phase were identified. It is evident that the resistance of glass-ceramics decreases as crystallization temperature increases, which could be attributed to a reduction in grain boundary resistance. According to the results (Fig.1), it could also be ascribed to a decrease in the proportion of the glass phase relative to the ceramic phase. Indeed, a residual glassy phase's resistance is frequently greater than that of a ceramic phase [29].

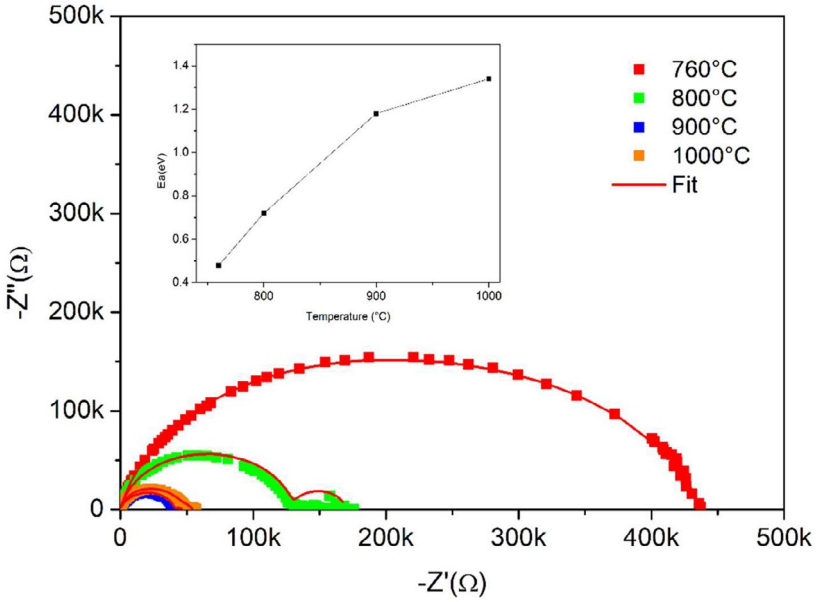


**Figure 7:** Impedance plots of the BNNWP crystallized at different temperatures, inset: the activation energy evolution versus the crystallization temperature

The relaxation activation energy ($E_a$) of polarization interfacial obtained by $lnr = lnr_0 \exp\left(\frac{Ea}{K_B T}\right)$ is illustrated in the inset of Fig.7. The Ea values of the B760, B800, B900, and KBT B1000 glass-ceramics were 0.48 eV, 0.72 eV, 1.18 eV, and 1.34 eV, respectively. It is observed that activation energy increases as crystallization temperature rises. This result could be owing to the highly resistant ceramic phase generated by a higher crystallization temperature [19]. It is worth noting that the glass phase exhibits a high BDS because it is nearly defect free. With an increase in ceramic phases, the glassy network was degraded, which decreased the BNNWP glass-ceramics electric breakdown strength. The increased amount of interfaces located between the glass and ferroelectric grains impeded the movement of space charges, leading to a higher $E_a$ [30]. Because of the enormous amount of charges accumulating, the risk of an electric field disruption increases. Consequently, the samples with high crystallization temperatures are more susceptible to breakdown.

### 3.4 Energy Storage Properties

The polarization–electric field (P–E) hysteresis loops of the samples, recorded at 1 kHz and room temperature, are illustrated in Fig. 8. As shown, the samples' P-E loops displayed linear dielectric behavior. In addition, it is noticed that polarization in8creases as crystallization temperature increases. For example, the maximum polarization passes from 0.55 to 0.77, 1.62, and 3.67 μC/cm$^2$ for B760, B800, B900, and B1000, respectively, at 120 kV/cm. This behavior is linked to the increase of dielectric constant with rising crystallization temperature, as demonstrated in Fig. 5.

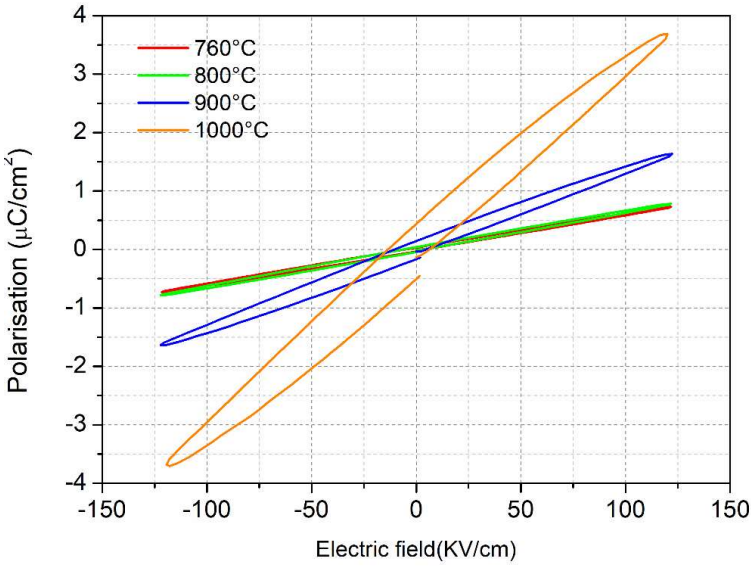


**Figure 8:** P-E hysteresis loops for BNNWP glass-ceramics at different temperatures under 120 kV/cm.

Figure 9 illustrates the variation in discharged energy density (Wrec) and energy efficiency (η) in response to different electric fields. Table 1 reports the dielectric and energy storage parameters of BNNWP glass-ceramics. It is noticed that the Wrec increases as the electric field strength increases. For instance, the Wrec of B900 increases from 21.5mJ/cm$^3$ at 60 kV/cm to 84.1mJ/cm3 at of 120 kV/cm. In addition, at a similar electric field of 120 kV/cm, the recoverable energy density was enhanced as the crystallization temperature increased. For instance, it passes from 41.1 mJ/cm3 for B760 to 177.3 mJ/cm3 for B1000. In reality, Wrec values calculated from P-E loops do not achieve their maximum value because 120 kV/cm (applied field) is far from BDS. Moreover, it is noticed that the energy efficiency of samples reduces as the applied electric field increases. This behavior may be ascribed to the conductivity increase as the applied electric field rises. However, the variance of the decreases is less than 3% for all samples, demonstrating that the evolution of η(%) versus the electric field is stable. Furthermore, it can be seen that increasing crystallization temperature results in reduced energy efficiency. It decreases from 88.5%, 87%, 80% and 73.8% for B760, B800, B900 and B1000, respectively, at 120kV/cm. This behavior could be explained by an increase in interfacial polarization at intersections between the glass phase and the ceramic phase, which is in agreement with the increase of Ea [20,31]. Because of increased polarization at interfaces, more stored charges cannot be released during the discharge process, leading to a loss in energy efficiency.

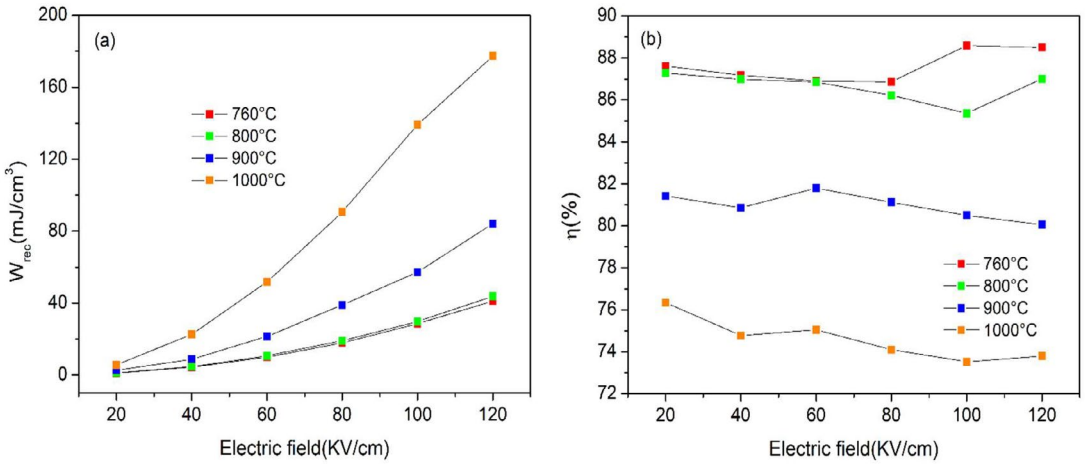


**Figure 9:** (a) Discharged energy density ($W_{rec}$) and (b) energy efficiency (η) of BNNWP glass-ceramics.

| T(°C) | $\varepsilon_r$ | Tanδ | $E_a$ (eV) | $W_{tot}$(mJ /cm$^3$) | $W_{rec}$(mJ /cm$^3$) | η(%) |
|---|---|---|---|---|---|---|
| 760 | 65 | 0.017 | 0.47 | 46.4 | 41.1 | 88.5 |
| 800 | 100 | 0.008 | 0.72 | 50.2 | 43.7 | 87 |
| 900 | 218 | 0.011 | 1.18 | 105.1 | 84.1 | 80 |
| 1000 | 315 | 0.038 | 1.34 | 240.2 | 177.3 | 73.8 |

**Table 1: Dielectric and energy storage parameters of BNNWP glass-ceramics**

## 4. Conclusion

In conclusion, the temperature of crystallization has a considerable effect on dielectric characteristics, energy storage properties, phase formation, and microstructure evolution. The precipitation of Ba2NaWNb4O15 and of NaNbO3 phases from the glass matrix was revealed by XRD analysis. In addition, the content of the forming phases increased as the crystallization temperature increased. The relative permittivity increases gradually with the crystallization temperature. The dielectric constant at room temperature increased from 65 to 315 as the heat treatment temperature increased from 760 to 1000 °C. This behavior was connected to the proportions of the phases and the increase in average grain size of BNNWP glass-ceramics. The dielectric study revealed that the samples showed good temperature stability. For the

crystallization temperature range of 760 °C to 900 °C the dielectric constant varies by less than 3% range of 25° to 250 °C. The sample heated at 1000 °C has a high Wrec of 177mJ/ cm3, combined with a dielectric constant of 315.


## Acknowledgments

The authors gratefully acknowledge the financial support of CNRST, OCP foundation, and the European Union's Horizon H2020-MSCA-RISE research and innovation actions,-ENGIMA and MELON.


## References


1. Hao, X. (2013). A review on the dielectric materials for high energy-storage application. *Journal of Advanced Dielectrics, 3*(01), 1330001.
2. Yao, Z., Song, Z., Hao, H., Yu, Z., Cao, M., Zhang, S., ... & Liu, H. (2017).Homogeneous/inhomogeneous-structured dielectrics and their energy-storage performances. *Advanced Materials, 29*(20), 1601727.
3. Peddigari, M., Palneedi, H., Hwang, G. T., & Ryu, J. (2019). Linear and nonlinear dielectric ceramics for high-power energy storage capacitor applications. *Journal of the Korean Ceramic Society, 56*(1), 1-23.
4. Chauhan, A., Patel, S., Vaish, R., & Bowen, C. R. (2015). Anti-ferroelectric ceramics for high energy density capacitors. *Materials, 8*(12), 8009-8031.

5. Zou, K., Dan, Y., Xu, H., Zhang, Q., Lu, Y., Huang, H., & He, Y. (2019). Recent advances in lead-free dielectric materials for energy storage. *Materials Research Bulletin, 113*, 190-201.
6. Sun, J., Luo, B., & Li, H. (2022). A review on the conventional capacitors, supercapacitors, and emerging hybrid Ion capacitors: Past, present, and future. *Advanced Energy and Sustainability Research, 3*(6), 2100191.
7. Liu, S., Shen, B., Hao, H., & Zhai, J. (2019). Glass–ceramic dielectric materials with high energy density and ultra-fast discharge speed for high power energy storage applications. *Journal of Materials Chemistry C, 7*(48), 15118-15135.
8. Chen, X., Tang, Y., Bo, X., Song, J., & Luo, J. (2018). Microstructures and energy storage properties of Sr 0.5 Ba 0.5 Nb 2 O 6 ceramics with SrO–B 2 O 3–SiO 2 glass addition. *Journal of Materials Science: Materials in Electronics, 29*, 17563-17570.
9. Peng, X., Pu, Y., Du, X., Ji, J., Gao, P., Zhang, L., & Sun, Z. (2021). Tailoring of ferroelectrics in (Na2O, K2O)-Nb2O5-SiO2 glass-ceramics via control the crystallization kinetics. *Chemical Engineering Journal, 422*, 130027.
10. Palneedi, H., Peddigari, M., Hwang, G. T., Jeong, D. Y., & Ryu, J. (2018). High-performance dielectric ceramic films for energy storage capacitors: progress and outlook. *Advanced Functional Materials, 28*(42), 1803665.
11. Pan, Z., Ding, J., Hou, X., Shi, S., Yao, L., Liu, J., ... & Pan, H. (2021). Substantially improved energy storage capability of ferroelectric thin films for application in high-temperature capacitors. *Journal of Materials Chemistry A, 9*(14), 9281-9290.
12. Peng, X., Pu, Y., Du, X., Ji, J., Zhou, S., & Zhang, L. (2020). The effect of glass network structure on interfacial polarization in Na2O–K2O–Nb2O5–SiO2–BaO glass-ceramics. *Journal of Alloys and Compounds, 845,* 155645.
13. Liu, C., Xie, S., Bai, H., Yan, F., Fu, T., Shen, B., & Zhai, J. (2022). Excellent energy storage performance of niobate-based glass-ceramics via introduction of nucleating agent. *Journal of Materiomics, 8*(4), 763-771.
14. Xie, S., Liu, C., Bai, H., Fu, T., Shen, B., & Zhai, J. (2022). Crystallization-temperature controlled alkali-free niobate glass-ceramics with high energy storage density and actual discharge energy density. *Journal of Alloys and Compounds, 910*, 164923.
15. Wang, S., Tian, J., Jiang, T., Zhai, J., & Shen, B. (2018). Effect of phase structures on dielectric properties and energy storage performances in Na2O-BaO-PbO-Nb2O5-SiO2-Al2O3 glass-ceramics. *Ceramics International, 44*(18), 23109-23115.
16. Song, Z., Liu, H., Zhang, S., Wang, Z., Shi, Y., Hao, H., ... & Yu, Z. (2014). Effect of grain size on the energy storage properties of (Ba0. 4Sr0. 6) TiO3 paraelectric ceramics. *Journal of the European Ceramic Society, 34*(5), 1209-1217.
17. Wang, S., Tian, J., Yang, K., Liu, J., Zhai, J., & Shen, B. (2018). Crystallization kinetics behavior and dielectric energy storage properties of strontium potassium niobate glass-ceramics with different nucleating agents. *Ceramics International, 44*(7), 8528-8533.
18. Chen, C., Zheng, Y., & Li, B. (2022). Achieving ultrafast discharge speed and excellent energy storage efficiency in environmentally friendly niobate-based glass ceramics. *Journal of the European Ceramic Society, 42*(15), 6977-6984.
19. Jiang, T., Chen, K., Shen, B., & Zhai, J. (2019). Excellent energy storage and charge-discharge performances in sodium-barium-niobium based glass ceramics. *Ceramics International, 45*(15), 19429-19434.
20. Chen, K., Jiang, T., Shen, B., & Zhai, J. (2021). Effects of crystalline temperature on microstructures and dielectric properties in BaO-Na2O-Bi2O3-Nb2O5-Al2O3-SiO2 glass-ceramics. *Materials Science and Engineering:* B, 263, 114885.
21. Ihyadn, A., Lahmar, A., Luk'Yanchuk, I., Mezzane, D., Bih, L., Alimoussa, A., & El Marssi, M. (2022). Structural, dielectric and energy storage properties of BaO–Na2O–Nb2O5–P2O5 glass-ceramics. *Physics and Chemistry of Glasses-European Journal of Glass Science and Technology Part B, 63*(2), 33-42.
22. Ihyadn, A., Lahmar, A., Mezzane, D., Bih, L., Alimoussa, A., Amjoud, M., ... & Luk'yanchuk, I. A. (2019). Structural, elelectrical and energy storage properties of BaO–Na2O–Nb2O5–WO3–P2O5 glass–ceramics system. *Materials Research Express, 6*(11), 115203.
23. Jiang, D., Zhong, Y., Shang, F., & Chen, G. (2020). Crystallization, microstructure and energy storage behavior of borate glass–ceramics. *Journal of Materials Science: Materials in Electronics, 31*, 12074-12082.
24. Neqali, A., Belboukhari, A., Bensaid, H., El Bouari, A., Bih, L., Alimoussa, A., ... & Mezzane, D. (2016). Diffuse phase transition and impedance spectroscopy analysis of Ba 2.15− x Na 0.7+ x Nb 5− x W x O 15 (x= 0.25) ferroelectric ceramic. *Applied Physics A, 122*, 1-8.
25. Bih, L., Bih, H., Amalhay, M., Mossadik, H., Elbouari, A., Belhorma, B., ... & Valente, M. A. (2014). Phosphate glass-glasses as new energy density dielectric materials. *Procedia Engineering, 83,* 371-377.
26. Zhou, Y., Qiao, Y., Tian, Y., Wang, K., Li, G., & Chai, Y. (2017). Improvement in structural, dielectric and energy-storage properties of lead-free niobate glass-ceramic with Sm2O3. *Journal of the European Ceramic Society, 37*(3), 995-999.
27. Wang, G., Lu, Z., Li, Y., Li, L., Ji, H., Feteira, A., ... & Reaney, I. M. (2021). Electroceramics for high-energy density capacitors: current status and future perspectives. *Chemical Reviews, 121*(10), 6124-6172.
28. Xue, S., Liu, S., Zhang, W., Shen, B., & Zhai, J. (2015). Correlation of energy conversion efficiency and interface polarization in niobate glass-ceramic for energy-storage applications. *Applied Physics Letters, 106*(16).
29. Wang, H., Liu, J., Zhai, J., Shen, B., Pan, Z., Yang, K., & Liu, J. (2017). Effect of K2O content on breakdown strength and energy-storage density in K2O-BaO-Nb2O5-SiO2 glass-ceramics. *Ceramics International, 43*(5), 4183-4187.
30. Zhang, Y., Wang, X. R., Song, X. Z., Ma, T., & Zhang, Q. (2012). Interfacial polarization arising from two contributions in glass added barium titanate ceramics.

*Journal of Materials Science: Materials in Electronics, 23*, 2301-2305.

31. Huang, J., Zhang, Y., Ma, T., Li, H., & Zhang, L. (2010). Correlation between dielectric breakdown strength and interface polarization in barium strontium titanate glass ceramics. *Applied Physics Letters, 96*(4).